Article

A Combined Computational and Experimental Study of Polynuclear Ru–TPPZ Complexes: Insight into the Electronic and Optical Properties of Coordination Polymers

Simona Fantacci, Filippo De Angelis, Jingjing Wang, Stefan Bernhard, and Annabella Selloni

J. Am. Chem. Soc., **2004**, 126 (31), 9715-9723• DOI: 10.1021/ja048421u • Publication Date (Web): 16 July 2004

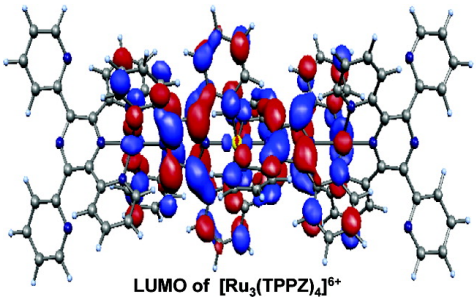

LUMO of $[Ru_3(TPPZ)_4]^{6+}$

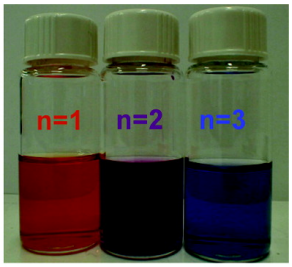

$[Ru_n(TPPZ)_{n+1}]^{2n+}$

More About This Article

Additional resources and features associated with this article are available within the HTML version:

- Supporting Information
- Links to the 8 articles that cite this article, as of the time of this article download
- Access to high resolution figures
- Links to articles and content related to this article
- Copyright permission to reproduce figures and/or text from this article

View the Full Text HTML

J|A|C|S
ARTICLES
Published on Web 07/16/2004

A Combined Computational and Experimental Study of Polynuclear Ru−TPPZ Complexes: Insight into the Electronic and Optical Properties of Coordination Polymers

Simona Fantacci,*[,†,‡] Filippo De Angelis,[†,‡] Jingjing Wang,[‡] Stefan Bernhard,*[,‡] and Annabella Selloni[‡]

Contribution from the Istituto CNR di Scienze e Tecnologie Molecolari (ISTM), Dipartimento di Chimica, Università di Perugia, via Elce di Sotto 8, I-06123, Perugia, Italy, and Department of Chemistry, Princeton University, Princeton, New Jersey 08544

Received March 19, 2004; E-mail: simona@thch.unipg.it; sbernhar@princeton.edu

Abstract: We report a combined experimental and computational study of polynuclear $[Ru_n(TPPZ)_{n+1}]^{2n+}$ complexes, of interest in the field of photoactive polymers. The complexes with $n = 1$, 2, 3 and $n > 5$ have been synthesized and spectroscopically characterized. A red-shift of the visible band maximum from 2.59 to 2.03 eV is observed going from the monomer to the longer oligomeric species ($n > 5$). To characterize the geometries, electronic structure, and excited states of these complexes, density functional theory (DFT) and time-dependent DFT calculations on the $[Ru_n(TPPZ)_{n+1}]^{2n+}$ series with $n = 1-4$ in solution have been performed. The agreement between experimental and calculated spectra is good, both in terms of absorption maximum energies and relative intensities for different values of *n*. For all the investigated complexes, we assign the main band in the visible region as a metal-to-metal plus ligand charge transfer (MMLCT) transition. The resulting excited states are delocalized throughout the entire complexes, as they originate from a superposition of π^*(TPPZ)-t_{2g}(Ru) states. The low-energy shoulder of the main visible absorption band, present in the experimental spectra for $n > 1$, is proposed to arise from spin-forbidden singlet−triplet transitions of similar MMLCT character, consistent with the observed enhancement of this feature in the spectra of the corresponding Os oligomers.

Introduction

Molecular wires, the most fundamental component of molecular electronics,[1] have become a main area of interest in contemporary chemistry, physics, and material science.[2] Many potential applications of molecular wires can be envisioned; TNT sensors[3] and organic light emitting diodes[4] are just two of many examples. Many techniques have been used to date to probe the electron-transfer rates and the conductivity through these linear molecules. With the rise of scanning tunneling microscopy (STM), it became possible to measure the conductivity of single molecules directly. Employing this technique, Weiss, Allara, and Tour were able to examine the conductance properties of single molecular wires that had been inserted at grain boundaries within a self-assembled monolayer of insulating dodecathiolate on gold.[5] Similarly, Abruña and co-workers studied the topology and electrochemistry of two-dimensional ordered arrays of one-dimensional chains composed of bridging ligands and Fe(II) or Co(II) metal ions.[6] Prior to the possibility of manipulating single molecules, charge transport in linear systems was studied with photoinduced electron transfer reactions in donor−spacer−acceptor-type molecules. This field of "photonic" molecular wires often utilizes long-lived excited states in metal complexes (Ru(II), Ir(III), Re(I), etc.) as electron donors which are connected to metal complexes with electron acceptor properties. A variety of bridging ligands, with spacers ranging from highly conjugated polyalkynes[7] to purely aliphatic adamantane units,[8] have been explored, and a review article comparing electron-transfer rates of a plethora of such molecular devices was published by Balzani et al.[9] An extension of the work on these dinuclear systems are the studies on coordination polymers composed of bridging ligands and metal centers. A variety of synthetic studies employing Ru(II), Cu(I), Ag(I), and Fe(II) metal ions have been published, and photovoltaic and electrochromic applications were studied.[10]

† ISTM-CNR, Perugia.
‡ Princeton University.

(1) Tour, J. M. *Acc. Chem. Res.* **2000**, *33*, 791.
(2) (a) Bunz, U. H. F. *Chem. Rev.* **2000**, *100*, 1605−1644. (b) Davis, W. B.; Svec, W. A.; Ratner, M. A.; Wasielewski, M. R. *Nature* **1998**, *396*, 60−63.
(3) Swager, T. M. *Acc. Chem. Res.* **1998**, *31*, 201−207.
(4) Malliaras, G. G.; Scott, J. C. The Chemistry, Physics and Engineering of Organic Light-Emitting Diodes. In *Semiconducting Polymers*; Hadziioannou, G., van Hutten, P. F., Eds.; Wiley-VCH: New York, Weinheim, 2000.
(5) (a) Cygan, M. T.; Dunbar, T. D.; Arnold, J. J.; Bumm, L. A.; Shedlock, N. F.; Burgin, T. P.; Jones, L., II; Allara, D. L.; Tour, J. M.; Weiss, P. S. *J. Am. Chem. Soc.* **1998**, *120*, 2721−2732. (b) Bumm, L. A.; Arnold, J. J.; Cygan, M. T.; Dunbar, T. D.; Burgin, T. P.; Jones, L., II; Allara, D. L.; Tour, J. M.; Weiss, P. S. *Science* **1996**, *271*, 1705−1707.
(6) (a) Bernhard, S.; Takada, K.; Diaz, D. J.; Abruña H. D.; Mürner, H. *J. Am. Chem. Soc* **2001**, *123*, 10265−10271. (b) Díaz, D. J.; Bernhard, S.; Storrier, G. D.; Abruña, H. D. *J. Phys. Chem. B* **2001**, *105*, 8746−8754.
(7) Barigelletti, F.; Flamigni, L. *Chem. Soc. Rev.* **2000**, *29*, 1.
(8) Balzani, V.; Barigelletti, F.; Belser, P.; Bernhard, S.; DeCola, L.; Flamigni, L. *J. Phys. Chem.* **1996**, *100*, 16786−16788.
(9) Balzani, V.; Juris, A.; Venturi, M.; Campagna, S.; Serroni, S. *Chem. Rev.* **1996**, *96*, 759−833.

A common structural feature of all molecular wires systems is that they are composed of monomeric subunits, which are concatenated to form oligomeric and polymeric molecules of a $(A)_n$ or $A(BA)_n$ topology. In an effort to engineer the properties of a molecular wire, it remains one of the foremost objectives to understand and subsequently control the factors that influence the electronic interactions among these building blocks. Additionally, the number of repeated units in a molecular wire strongly influences its electronic structure, which is an observation that is uncommon in macroscopic wires and is not yet well-understood. To investigate these questions Osuka and coworkers synthesized porphyrin polymers and tapes to determine the effective conjugation chain length (ECL).[11] The ECL defines the extent of conjugation in a polymer, at which point the optical (electrochemical) properties reach a saturation level that is common with the corresponding oligomer[12] and can be evaluated from a plot of the longest wavelength absorption energy (redox potential) vs the inverse number of monomer units. The background of this plot is a "particle in a box" model, and it usually exhibits linearity at small degrees of polymerization. However, for longer chain lengths a saturation behavior can be observed, which in turn defines the ECL.

Because of the complexity of the synthetic paths employed to prepare these polymeric systems, it would be highly desirable to predict the electronic properties with suitable calculations. Yamaguchi used time-dependent density functional theory (TDDFT)[13] to investigate the electronic structure of porphyrin tapes and arrays similar to the ones synthesized by Osuka.[14] Numerous calculations of the current flowing through organic molecules and oligomers have been published.[15] DFT,[16] TDDFT,[17−20] and ab initio[21] computational studies of the absorption spectra of coordination complexes containing a single ruthenium center have been recently reported. With a few exceptions,[22−25] however, little theoretical work has been done to date on polynuclear coordination complexes to understand the interplay between metal ions and bridging ligands in coordination polymers. Experiments show that the nature of the metal center as well as the degree of delocalization within the bridging ligands strongly influence the optical and electronic properties of the resulting polymer, but theoretical accounts of these observations are not available yet.

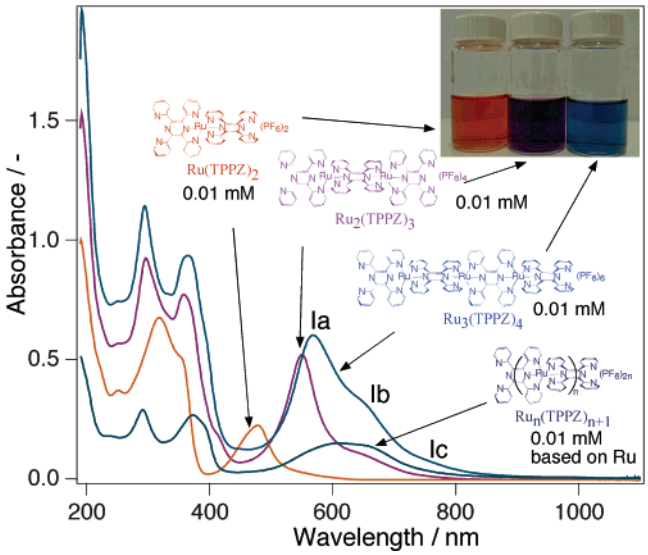

Figure 1. UV−vis of $[Ru(TPPZ)_2]^{2+}$, $[Ru_2(TPPZ)_3]^{4+}$, $[Ru_3(TPPZ)_4]^{6+}$, and $[Ru_n(TPPZ)_{n+1}]^{2n+}$ in acetonitrile (10 μM). Inset: Photograph of the complexes in acetonitrile solution (0.1 mM).

The work presented herein is a combined experimental and theoretical effort toward a comprehensive description of a ruthenium(II) coordination polymer which has potentially interesting molecular wire properties. On the experimental side, we have synthesized and characterized mononuclear $[Ru(TPPZ)_2]^{2+}$, dinuclear $[Ru_2(TPPZ)_3]^{4+}$, and trinuclear $[Ru_3(TPPZ)_4]^{6+}$ ruthenium(II) complexes (Figure 1) with the strongly coupled tetra-2-pyridylpyrazine (TPPZ) ligand, and we have also compared these oligomeric coordination compounds to a Ru(II)−TPPZ polymer $[Ru_n(TPPZ)_{n+1}]^{2n+}$. The synthesis and characterization of the mononuclear and dinuclear $[Ru(TPPZ)_2]^{2+}$ and $[Ru_2(TPPZ)_3]^{4+}$ species have been reported in the literature.[26] On the theoretical side, we have carried out a full quantum mechanical investigation of the geometry, electronic structure, and optical absorption spectra of the oligomers with n ranging from 1 to 4, using DFT and TDDFT calculations. The electronic absorption spectra of the investigated complexes have been measured and compared to the excitation energies and oscillator strengths obtained from TDDFT calculations in solution. On the basis of this comparison, the character of the observed bands was identified, and their assignment to various types of electronic transitions was made.

Experimental Section

The synthetic procedures and the characterization of the $[Ru_n(TPPZ)_{n+1}]^{2n+}$ complexes are reported in the Supporting Information. The synthetic procedures to prepare the TPPZ ligand are described elsewhere.[27] The experimental UV−vis absorption spectra of a 10 μM solution of the $[Ru_n(TPPZ)_{n+1}]^{2n+}$ complexes with $n = 1$, 2, 3 and $n > 5$ in acetonitrile are shown in Figure 1. The spectra exhibit two distinct features: (i) an absorption band in the visible region whose position undergoes a red-shift upon increasing the length of the coordination

(10) (a) Velten, U.; Lahn, B.; Rehahn, M. *Macromol. Chem. Phys.* **1997**, *198*, 2789−2816. (b) Velten, U.; Rehahn, M. *Macromol. Chem. Phys.* **1998**, *199*, 127−140. (c) Velten, U.; Rehahn, M. *Chem. Commun.* **1996**, 2639−2640. (d) Ng, W. Y.; Chan, W. K. *Adv. Mater.* **1997**, *9*, 716. (e) Yu, L.; Wang, Q. *J. Am. Chem. Soc.* **2000**, *122*, 11806−11811.
(11) Tsuda, A.; Osuka, A. *Science* **2001**, *293*, 79−82.
(12) Martin, R. E.; Diederich, F. *Angew. Chem., Int. Ed.* **1999**, *38*, 1351.
(13) Casida, M. Time Dependent Density Functional Response Theory for Molecules. In *Recent Advances in Density Functional Methods*; Chong, D. P., Ed.; World Scientific: Singapore, 1995; Vol. 1, p 155.
(14) Yamaguchi, Y. *J. Chem. Phys.* **2002**, *117*, 9688−9694.
(15) (a) Nitzan, A.; Ratner, M. A. *Science* **2003**, *300*, 1384 and references therein. (b) Kushmerick, J. G.; Holt, D. B.; Pollack, S. K.; Ratner, M. A.; Yang, J. C.; Schull, T. L.; Naciri, J.; Moore, M. H.; Shashidhar, R. *J. Am. Chem. Soc.* **2002**, *124*, 10654 and references therein.
(16) Daul, C.; Baerends, E. J.; Vernooijs, P. *Inorg. Chem.* **1994**, *33*, 3538.
(17) Monat, J. E.; Rodriguez, J. H.; McCusker, J. K. *J. Phys. Chem. A* **2002**, *106*, 7399−7406.
(18) Zabri, H.; Gillaizeau, I.; Bignozzi, C. A.; Caramori, S.; Charlot, M.-F.; Cano-Boquera, J.; Odobel, F. *Inorg. Chem.* **2003**, *42*, 6655−6666.
(19) Guillemoles, J.-F.; Barone, V.; Joubert, L.; Adamo, C. *J. Phys. Chem. A* **2002**, *106*, 11354−11360.
(20) (a) Fantacci, S.; De Angelis, F.; Selloni, A. *J. Am. Chem. Soc.* **2003**, *125*, 4381−4387. (b) De Angelis, F.; Fantacci, S.; Selloni, A. *Chem. Phys. Lett.* **2004**, 389, 204.
(21) (a) Cacelli, I.; Ferretti, A. *J. Chem. Phys.* **1998**, 109, 8583−8590. (b) Cacelli, I.; Ferretti, A. *J. Phys. Chem. A* **1999**, 103, 4438−4445.
(22) Cacelli, I.; Ferretti, A.; Toniolo, A. *J. Phys. Chem A* **2001**, *105*, 4480−4487.
(23) Marcaccio, M.; Paolucci, F.; Paradisi, C.; Roffia, S.; Fontanesi, C.; Yellowlees, L. J.; Serroni, S.; Campagna, S.; Denti, G.; Balzani, V. *J. Am. Chem. Soc.* **1999**, *121*, 10081−10091.
(24) Yutaka, T.; Mori, I.; Kurihara, M.; Mitzutani, J.; Kubo, K.; Furusho, S.; Mastumura, K.; Tamai, N.; Nishihara, H. *Inorg. Chem.* **2001**, *40*, 4986−4995.
(25) Bencini, A.; Ciofini, I.; Daul, C. A.; Ferretti A. *J. Am. Chem. Soc.* **1999**, *121*, 11418−11424.
(26) Arana, C. R.; Abruña, H. D. *Inorg. Chem.* **1993**, *32*, 194−203.
(27) Goodwin, H. A.; Lions, F. *J. Am. Chem. Soc.* **1959**, *81*, 6415−6422.

polymers and is responsible for the dramatic color changes and (ii) an absorption in the UV region of the spectrum which resolves into two distinct features with increasing *n*.

Theoretical Section

A. Computational Details. Geometry optimizations of $[Ru_n(TPPZ)_{n+1}]^{2n+}$ species with $n = 1-4$ were performed by means of DFT calculations within the Car–Parrinello (CP) method,[28] using a periodic supercell approach and no symmetry constraints. The parallel version[29] of the CP code with Vanderbilt pseudopotentials[30,31] was used. The generalized gradient approximation (GGA) was adopted by adding the exchange and correlation gradient corrections from ref 32 to the Perdew–Zunger LDA parametrization.[33] Core states were projected out using pseudopotentials. For all the atoms, "ultra-soft" pseudopotentials were generated according to the scheme proposed by Vanderbilt.[31] The wave functions and electron density were expanded in plane waves up to an energy cutoff of 25 and 200 Ry, respectively. A tetragonal supercell was used, with $16 \times 16 \times 21$, $16 \times 16 \times 28$, $16 \times 16 \times 35$, and $16 \times 16 \times 41$ Å^3 volume for the monomer (93 atoms), dimer (140 atoms), trimer (187 atoms), and tetramer (234 atoms), respectively. A minimum distance of 5.0 Å between repeated images was maintained.

The electronic structure and the TDDFT singlet excitation energies of the four $[Ru_n(TPPZ)_{n+1}]^{2n+}$ ($n = 1-4$) complexes in acetonitrile solution were computed taking into account solvation effects by means of the conductor polarizable continuum model (C-PCM).[34] The inclusion of solvation effects has been recently shown to be crucial when describing the electronic structure and absorption spectra of polypyridyl ruthenium complexes.[20] TDDFT calculations were performed on the CP-optimized geometries using the Gaussian03 (G03) program package,[35] which implements the nonequilibrium version[36] of the C-PCM algorithm. We note that in the present G03 implementation, dispersion–repulsion contributions to solvent shifts are identical for different electronic states. The B3LYP exchange-correlation functional[37] has been used for all the G03 calculations. To check the consistency of the CP/GGA and G03/B3LYP calculations, we compared the geometries of the monomer complex optimized at both levels of theory (for the G03 geometry optimization, the LANL2DZ basis set[38,39] was used, see Supporting Information). We found that the critical Ru–N bond distances and the pyrazine N–C–C–N dihedral angles computed by the two methods show maximum differences of 0.026 Å and 0.5°, respectively.

We investigated the effect of basis set expansion on the TDDFT excitation energies and oscillator strengths, considering both a minimal all-electron STO-3G basis[40] and a double-ζ LANL2DZ basis set[38,39] along with the corresponding pseudopotential for ruthenium. By comparing TDDFT results for $[Ru_n(TPPZ)_{n+1}]^{2n+}$ ($n = 1$, 2) obtained in vacuo with the two different basis sets, we found that the STO-3G basis set provides excitation energies and oscillator strengths comparable to those given by the larger LANL2DZ basis set (see the Supporting Information): the overall computed spectral shape is the same, apart from a quasi-rigid blue-shift of the LANL2DZ excitation energies with respect to those obtained with STO-3G. In particular, the main absorption feature in the visible region for the monomer (dimer) is found at 2.54 (2.17) and 2.82 (2.40) eV with the STO-3G and LANL2DZ basis sets, respectively, while intensity ratios of 2.6 between the main visible absorption maxima of the monomer and dimer are computed with both basis sets. Moreover, the dimer spectra computed with both basis sets show the presence of low intensity bands 0.7–0.9 eV below the main absorption maxima, with no other absorptions of relevant intensity between these two features. On the basis of the agreement between the results for the monomer and dimer spectra, we employed the minimal STO-3G basis set for all the calculations reported hereafter. Incidentally, we remark that TDDFT calculations for the $[Ru_n(TPPZ)_{n+1}]^{2n+}$ species with $n = 3$ and 4 would be computationally unaffordable with the larger LANL2DZ basis set.

B. Atomic Structure. In Figure 2, the optimized geometrical structures of the $[Ru_n(TPPZ)_{n+1}]^{2n+}$ complexes ($n = 1-4$) are shown together with relevant structural parameters. Further geometrical parameters are collected as Supporting Information. The ruthenium centers are oriented along the *z* axis, which therefore represents the growing axis of the molecular wire. For $n > 1$, we hereafter adopt the labeling of the TPPZ units reported in Figure 2.

The monomeric complex shows an intrinsic C_2 symmetry, with the Ru–N pyrazine bonds oriented along the *z* axis, slightly shorter than the Ru–N pyridyl ones (1.98 versus 2.07 Å). The optimized structure is characterized by a twisting of the pyrazine ligands, which results in a N–C–C–N dihedral angle of 19°, with the terminal pyridyl ligands following this distortion (this dihedral angle would be 0° for a completely planar geometry). A similar twisting is found for all the investigated complexes, while an almost perfect octahedral coordination of the $Ru-N_6$ core is computed.

For the dimer, we find a Ru–Ru distance of 6.75 Å, with the central pyrazine Ru–N bond lengths of TPPZ B slightly shorter (2.00 Å) than those involving the terminal pyrazines (2.10 Å). The central TPPZ B pyrazine N–C–C–N dihedral

(28) Car, R.; Parrinello, M. *Phys. Rev. Lett.* **1985**, *55*, 2471.
(29) Giannozzi, P.; De Angelis, F.; Car, R. *J. Chem. Phys.* **2004**, *120*, 5903.
(30) (a) Pasquarello, A.; Laasonen, K.; Car, R.; Lee, C.; Vanderbilt, D. *Phys. Rev. Lett.* **1992**, *69*, 1982. (b) Pasquarello, A.; Laasonen, K.; Car, R.; Lee, C.; Vanderbilt, D. *Phys. Rev. B* **1993**, *47*, 10142.
(31) Vanderbilt, D. *Phys. Rev. B* **1990**, *41*, 7892.
(32) Perdew, J. P.; Chevary, J. A.; Vosko, S. H.; Jackson, K. A.; Pederson, M. R.; Singh, D. J.; Fiolhais, C. *Phys. Rev. B* **1992**, *46*, 6671.
(33) Perdew, J. P.; Zunger, A. *Phys. Rev. B* **1981**, *23*, 5048.
(34) (a) Barone, V.; Cossi, M. *J. Phys Chem. A* **1998**, *102*, 1995. (b) Cossi, M.; Rega, N.; Scalmani, G.; Barone, V. *J. Comput. Chem.* **2003**, *24*, 669.
(35) Frisch, M. J.; Trucks, G. W.; Schlegel, H. B.; Scuseria, G. E.; Robb, M. A.; Cheeseman, J. R.; Montgomery, J. A., Jr.; Vreven, T.; Kudin, K. N.; Burant, J. C.; Millam, J. M.; Iyengar, S. S.; Tomasi, J.; Barone, V.; Mennucci, B.; Cossi, M.; Scalmani, G.; Rega, N.; Petersson, G. A.; Nakatsuji, H.; Hada, M.; Ehara, M.; Toyota, K.; Fukuda, R.; Hasegawa, J.; Ishida, M.; Nakajima, T.; Honda, Y.; Kitao, O.; Nakai, H.; Klene, M.; Li, X.; Knox, J. E.; Hratchian, H. P.; Cross, J. B.; Adamo, C.; Jaramillo, J.; Gomperts, R.; Stratmann, R. E.; Yazyev, O.; Austin, A. J.; Cammi, R.; Pomelli, C.; Ochterski, J. W.; Ayala, P. Y.; Morokuma, K.; Voth, G. A.; Salvador, P.; Dannenberg, J. J.; Zakrzewski, V. G.; Dapprich, S.; Daniels, A. D.; Strain, M. C.; Farkas, O.; Malick, D. K.; Rabuck, A. D.; Raghavachari, K.; Foresman, J. B.; Ortiz, J. V.; Cui, Q.; Baboul, A. G.; Clifford, S.; Cioslowski, J.; Stefanov, B. B.; Liu, G.; Liashenko, A.; Piskorz, P.; Komaromi, I.; Martin, R. L.; Fox, D. J.; Keith, T.; Al-Laham, M. A.; Peng, C. Y.; Nanayakkara, A.; Challacombe, M.; Gill, P. M. W.; Johnson, B.; Chen, W.; Wong, M. W.; Gonzalez, C.; Pople, J. A. *Gaussian 03*, revision B.01; Gaussian, Inc.: Pittsburgh, PA, 2003.
(36) Cossi, M.; Barone, V. *J. Chem. Phys.* **2001**, *115*, 4708.
(37) Becke, A. D. *J. Chem. Phys.* **1993**, *98*, 5648.
(38) Dunning, T. H., Jr.; Hay, P. J. In *Modern Theoretical Chemistry*; Schaefer, H. F., III, Ed.; Plenum: New York, 1976; Vol. 3, pp 1–28.
(39) (a) Hay, P. J.; Wadt, W. R. *J. Chem. Phys.* **1985**, *82*, 270. (b) Wadt, W. R.; Hay, P. J. *J. Chem. Phys.* **1985**, *82*, 284. (c) Hay, P. J.; Wadt, W. R. *J. Chem. Phys.* **1985**, *82*, 299.
(40) (a) Hehre, W. J.; Stewart, R. F.; Pople, J. A. *J. Chem. Phys.* **1969**, *51*, 2657. (b) Collins, J. B.; Schleyer, P. v. R.; Binkley, J. S.; Pople, J. A. *J. Chem. Phys.* **1976**, *64*, 5142.

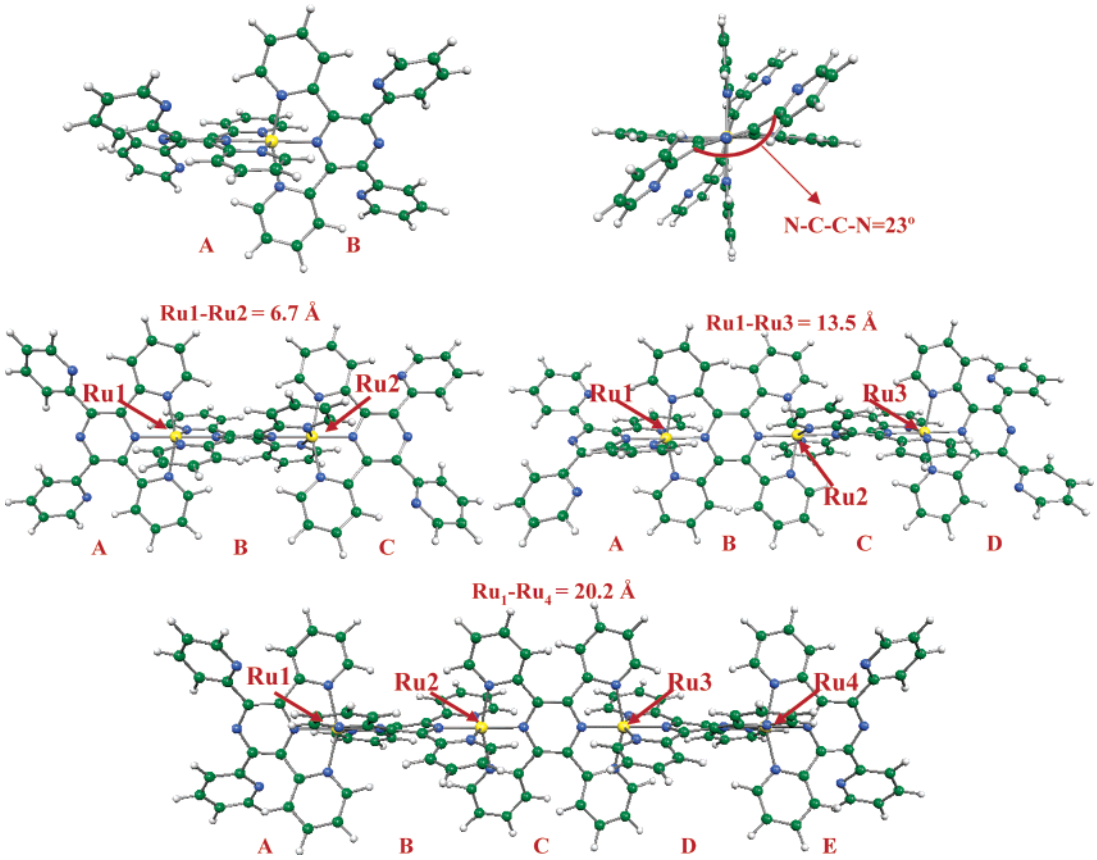

Figure 2. Optimized molecular structure of $[Ru_n(TPPZ)_{n+1}]^{2n+}$ complexes with $n = 1-4$.

angle is about 18°, whereas those of the terminal pyrazines (TPPZs A and C) show values close to 24°.

The trimer complex shows a pseudo-rotoreflection center coinciding with the central ruthenium atom. The pyrazine Ru1−N (TPPZ B) and Ru3−N (TPPZ C) bond lengths are slightly shorter (1.98 Å) than those of the remaining pyrazine Ru−N bond lengths, which have all similar values (2.02−2.03 Å). Both Ru−Ru distances are 6.75 Å, the same value found in the dimeric complex, and also in this case the twisting of terminal pyrazine rings is more pronounced with respect to that of the central ligands (∼23° versus ∼18°).

A bond alternation similar to that found for the trimer is present for the tetramer, with pyrazine Ru1−N (TPPZ B) and Ru4−N (TPPZ D) bond distances (1.97 Å) slightly shorter than the remaining ones (2.00−2.02 Å). The terminal pyrazine N−C−C−N dihedral angles are ∼23°, and this dihedral angle decreases going toward the central part of the molecule where it takes values of ∼18°, and ∼15°. Intermetallic distances close to 6.7 Å are computed in this case too, with a Ru1−Ru4 distance of 20.2 Å and N−N distances between the terminal pyrazines close to 30 Å. The computed geometrical parameters suggest that the rigid TPPZ ligand ensures a strict control over the metal−metal distances throughout the investigated series.[41]

C. Electronic Structure in Solution. The energy and character of the frontier orbitals of the four investigated ruthenium complexes in acetonitrile are summarized in Figure 3 and detailed in the Supporting Information. The general trend is that the first LUMOs are π^* orbitals delocalized on the TPPZ ligands with sizable contributions from the ruthenium centers, whereas the HOMOs are the ruthenium t_{2g} orbitals, with the four nitrogen lone pairs of the terminal pyridyl groups lying at lower energies.

Monomer. For the monomeric $[Ru(TPPZ)_2]^{2+}$ complex, the HOMO, HOMO-1, and HOMO-2 (orbitals 223, 222, and 221, respectively) are quasi-degenerate ruthenium t_{2g} orbitals of nonbonding character. The four nitrogen lone pairs of the terminal pyridyl rings (orbitals 220−217) constitute a quasi-degenerate set and lie 0.84 eV below the HOMOs (Figure 3). The LUMOs are a set of four π^* orbitals lying 2.73 eV above the HOMO in a 0.36 eV energy interval (orbitals 224−227) and are symmetrically delocalized over the two pyrazine rings of TPPZs A and B. In particular, orbitals 225 and 227 are antibonding combinations of Ru $d_{xz} - d_{yz}$ and pyrazine nitrogen $p_x - p_y$ orbitals, with Ru contributions up to 22%. A second set of four orbitals of pure π^* character (orbitals 228−231), essentially delocalized over the pyridyl rings of both TPPZ ligands, is present ∼1.1 eV above the first set of LUMOs.

Dimer. For the $[Ru_2(TPPZ)_3]^{4+}$ dimeric complex, the first five HOMOs (orbitals 345−341), lying in a range of 0.34 eV (Figure 3), are nonbonding combinations of Ru t_{2g} orbitals localized on both metal centers (see HOMO and HOMO-1 in Figure 4). The four nitrogen lone pairs of the terminal pyridyls of TPPZs A and C lie ∼0.4 eV below orbital 341. The sixth orbital with metal character (orbital 336, also shown in Figure 4) is 0.89 eV below the HOMO and results from the π bonding interaction between the t_{2g} orbitals of both ruthenium centers and the pyrazine nitrogen p orbitals of the central TPPZ B

(41) De Cola, L.; Belser, P. *Coord. Chem. Rev.* **1998**, *177*, 301−346.

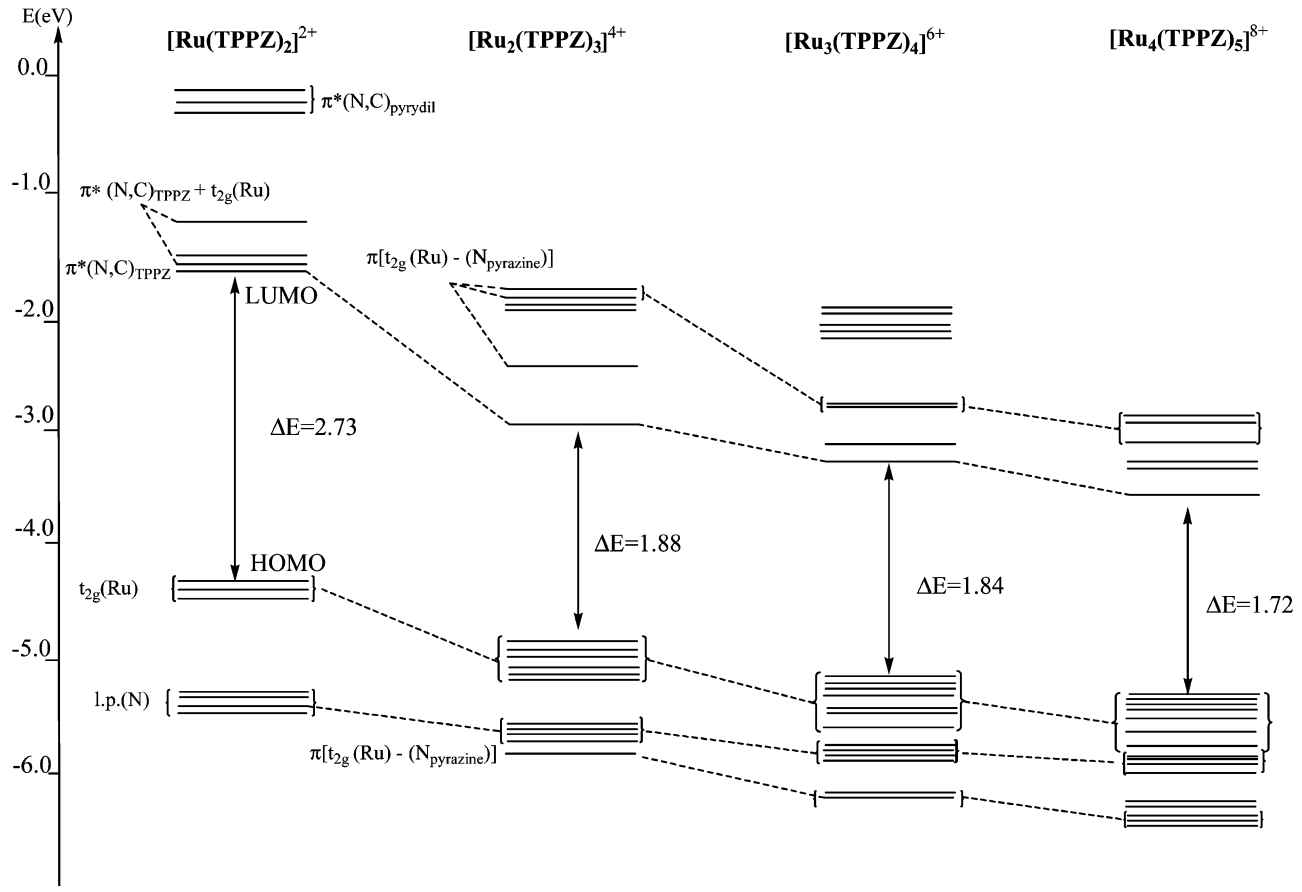

Figure 3. Energy levels (eV) of $[Ru_n(TPPZ)_{n+1}]^{2n+}$ complexes with $n = 1-4$ in acetonitrile.

ligand. This bonding interaction, taking place in the plane orthogonal to the central pyrazine ring, is responsible for the stabilization of orbital 336 with respect to the remaining t_{2g} HOMOs. Such an orbital interaction is missing in the monomer and is related to intermetal communication through the pyrazine bridging ligand. Experimental evidence of this intermetal communication was provided by Arana and Abruña,[26] who observed the existence of two distinct one-electron oxidations for the $[Ru_2(TPPZ)_3]^{4+}$ dimeric complex at +1.53 and +0.99 V, while a symmetric noninteracting dimer would exhibit metal-based oxidation at the same potential for both metal centers. This pyrazine-mediated intermetal communication is found also in the $[Ru_3(TPPZ)_4]^{6+}$ and $[Ru_4(TPPZ)_5]^{8+}$ species, where it gives rise to stabilization of two and three Ru pyrazine bonding orbitals, respectively (see Figure 3).

The dimer LUMO (orbital 346), which is 1.87 eV above the HOMO, is a π^* orbital mainly localized on the carbon atoms of the central TPPZ ligand, with small percentages (about 10%) of metal orbitals. This orbital is stabilized with respect to the monomer LUMO by ~1.3 eV, whereas the analogous stabilization of the HOMO is ~0.46 eV. Thus, the smaller HOMO–LUMO gap that we find for the dimer (1.87 eV) with respect to the monomer (2.73 eV) is essentially due to the LUMO stabilization, which reflects the TPPZ π^* stabilization upon coordination to a second metal center. Interestingly, this difference in stabilization between the HOMO and the LUMO may be related to the experimentally observed redox behavior of the monomer and dimer complexes, showing an almost constant value of the first (metal-based) oxidation potential (+1.50 V for the monomer vs +1.53 V for the dimer) and a change of the first (ligand-based) reduction potential (−0.88 V for the monomer vs −0.29 V for the dimer).[26]

At higher energy, 0.47 eV above the LUMO, the LUMO+1 (orbital 347 in Figure 4) is the antibonding partner of orbital 336 and shows a 35% contribution of ruthenium t_{2g} orbitals, arising from both metal centers, mixed with a comparable percentage of the central pyrazine (TPPZ B) nitrogen p orbitals. The LUMO+2 and LUMO+3 (orbitals 348 and 349) are almost degenerate orbitals lying 0.46 eV above the LUMO+1 and are completely delocalized on both the pyrazine and pyridyl ligands of the external TPPZs A and C, respectively, showing negligible contribution of metal orbitals. The LUMO+4 and LUMO+5 (orbitals 350 and 351 in Figure 4), which have metal orbital percentages of ~14%, are t_{2g}-π^* antibonding combinations delocalized over TPPZs A and C, respectively, involving a single ruthenium center and the pyrazine nitrogens.

Trimer and Tetramer. An orbital pattern similar to that for the $[Ru_2(TPPZ)_3]^{4+}$ species is found for the HOMOs and LUMOs of the $[Ru_3(TPPZ)_4]^{6+}$ and $[Ru_4(TPPZ)_5]^{8+}$ oligomers. The intermetal communication in these trimeric and tetrameric species takes place among pairs of contiguous metal centers, since the bridging pyrazine ligands involved in such interactions lie in orthogonal planes as a result of the octahedral environment imposed by the ruthenium(II) center.

The first HOMOs of $[Ru_3(TPPZ)_4]^{6+}$ and $[Ru_4(TPPZ)_5]^{8+}$ are seven and nine nonbonding t_{2g} orbitals, respectively, followed in order of decreasing energy by the four nitrogen lone pairs of the terminal pyridyl ligands, with two (orbitals 455 and 456) and three (orbitals 572, 575 and 576) bonding combinations, respectively, of Ru t_{2g} and pyrazine nitrogen orbitals being

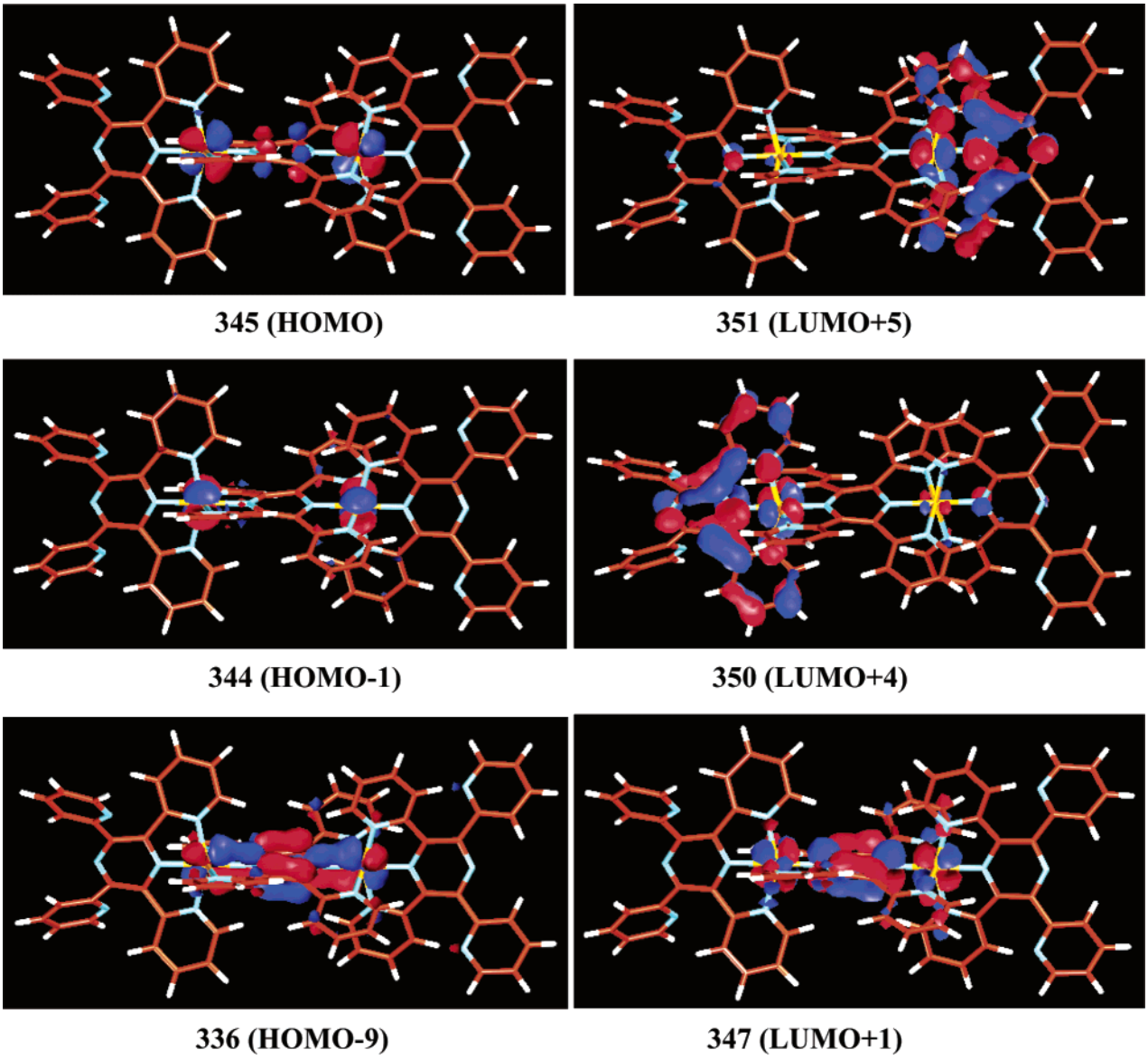

Figure 4. Isodensity surface plot (isodensity contour = 0.03) of the 347 (LUMO+1), 350 (LUMO+4), 351 (LUMO+5), 345 (HOMO), 344 (HOMO-1), and 336 (HOMO-9) orbitals of $[Ru_2(TPPZ)_3]^{4+}$ complex.

stabilized and lying about 0.9−1.0 eV below the HOMO (Figure 3). The LUMO of $[Ru_3(TPPZ)_4]^{6+}$ is a π^* orbital essentially delocalized on the carbon atoms of the central TPPZs (B and C) ligands, while for $[Ru_4(TPPZ)_5]^{8+}$ such a π^* LUMO is delocalized over the central TPPZ C ligand only, as in the dimer case. In the trimer, the LUMO+2 and LUMO+3 corresponding to orbitals 470 and 471, are the antibonding counterpart of orbitals 455 and 456 and lie about 0.5 eV above the LUMO. In the tetramer, orbitals of similar character (orbitals 593−595) lie 0.5 to 0.6 eV above the LUMO (orbital 590); however, the LUMO+1 and LUMO+2 also have nonnegligible amounts of metal character (11−15%).

The ruthenium t_{2g} HOMOs are stabilized by 0.39 eV going from the dimer to the trimer and by 0.17 eV from the trimer to the tetramer. At the same time, the LUMO of $[Ru_3(TPPZ)_4]^{6+}$ is stabilized by 0.42 eV with respect to that of the dimeric $[Ru_2(TPPZ)_3]^{4+}$ species, while the LUMO of the $[Ru_4(TPPZ)_5]^{8+}$ oligomer is still 0.28 eV lower in energy (Figure 3). The resulting HOMO−LUMO gaps are 1.84 and 1.72 eV for the $[Ru_3(TPPZ)_4]^{6+}$ and $[Ru_4(TPPZ)_5]^{8+}$ oligomers, respectively. Thus, the largest HOMO−LUMO gap reduction takes place going from the monomer to the dimer, while the gap reductions become increasingly smaller from $n = 2$ on.

UV−vis Spectra: Comparison between Theory and Experiment

A. Monomer. A comparison of the experimental spectrum of the monomer with that computed for the $[Ru(TPPZ)_2]^{2+}$ complex in acetonitrile is presented in Figure 5. The experimental spectrum of the monomer in acetonitrile shows three main spectral features below 4.0 eV (we hereafter report spectral data in eV), labeled in order of increasing energy as I, II, and III, respectively: a band in the visible at 2.59 eV (I), a more intense band in the UV region at 3.89 eV (III), and a pronounced shoulder of band III at 3.52 eV (II) (Figures 1 and 5). The agreement between the two spectra is good, both in terms of band positions, relative intensity, and overall spectral shape, especially considering the limited size of the basis set used for

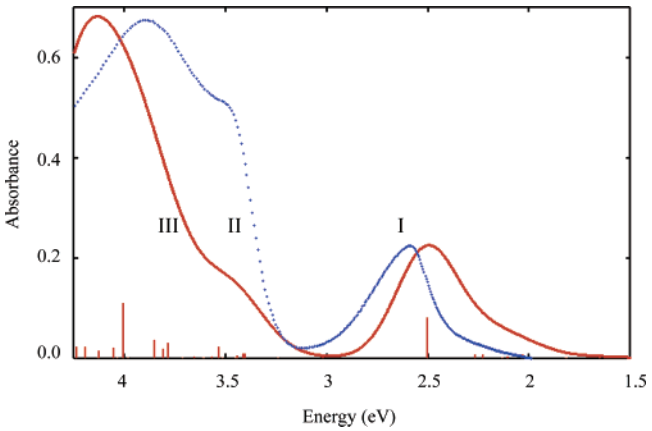

Figure 5. Comparison between the experimental (blue line) and computed (red line) spectrum of the monomeric $[Ru(TPPZ)_2]^{2+}$ in acetonitrile (energy in eV). Computed oscillator strengths have been rescaled so that the intensity of the first absorption band (I) of the experimental and calculated spectra match. Red vertical lines correspond to unbroadened excitation energies and rescaled oscillator strengths.

the calculations. The computed peak positions of the three bands agree within 0.1 eV with the experiment, and only the relative intensity of band II is underestimated.

Detailed analysis of the calculated spectrum shows that band I is composed by an intense transition at 2.51 eV followed by a series of five weaker transitions forming the band tail below 2.5 eV (see Supporting Information). All these transitions originate from combinations of the Ru t_{2g} HOMOs (orbitals 223−221) but involve different final orbitals. In particular, the excited state giving rise to the intense transition at 2.51 eV is mainly composed of orbitals 225 and 227, which, on the basis of the monomer's electronic structure discussed above, have t_{2g}-π^* character and are delocalized over both the pyridyl and pyrazine ligands (except the terminal pyridyl rings) of the two TPPZ units, with sizable contributions of ruthenium d orbitals. We therefore assign band I as a metal-to-metal plus ligand charge transfer (MMLCT) transition. On the other hand, the final states of the less intense transitions giving rise to the band tail are mainly orbitals 224 and 226, which have almost vanishing metal character. Thus, we can relate the higher intensity of the transition at 2.51 eV to the presence of metal orbitals in the final states.

At higher energies (3.53 eV in the computed spectrum), shoulder II is assigned to have pure metal-to-ligand charge transfer (MLCT) character: it essentially originates from transitions starting from the Ru t_{2g} HOMO and arriving at π^* orbitals delocalized over the pyridyl ligands (orbitals 228−231). Finally, band III originates from a series of intense transitions dominated by a strong absorption at 4.03 eV, for which the starting states are a set of π bonding orbitals delocalized over the TPPZ ligands (orbitals 211−216), while the final states are the 224−227 orbitals. This band is therefore composed by $\pi-\pi^*$ transitions, with variable amounts of metal character in the arriving states. It is worth noting that even though band II appears as a shoulder of band III in the experimental and theoretical spectra, these two features are computed to have completely different character. Indeed, in the experimental spectra this difference is enhanced with increasing n, so that shoulder II becomes a well-defined band for oligomers with $n > 2$ (see Figure 1).

Table 1. Computed Absorption Energies (eV) and Relative Intensities (in Parentheses) of the Ia Absorption Maxima Compared to the Available Experimental Values

	theor	exptl
$Ru(TPPZ)_2^{2+}$	2.50 (1.0)	2.59 (1.0)
$Ru_2(TPPZ)_3^{4+}$	2.10 (2.1)	2.25 (2.2)
$Ru_3(TPPZ)_4^{6+}$	1.91 (3.3)	2.18 (2.7)
$Ru_4(TPPZ)_5^{8+}$	1.82 (4.6)	
$Ru_{5.5}(TPPZ)_{6.5}^{10+}$ (oligomer)		2.03 (3.3)

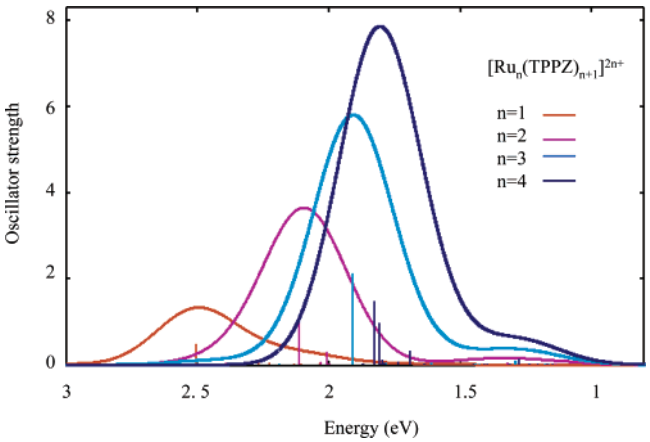

Figure 6. Computed spectra of $[Ru_n(TPPZ)_{n+1}]^{n+}$ complexes with $n = 1$ (red line), 2 (violet line), 3 (blue line), and 4 (deep blue line) (energy in eV). Vertical lines correspond to unbroadened excitation energies and oscillator strengths.

B. Dimer, Trimer, and Tetramer Spectra in the Visible Region. The experimental spectra of the investigated $[Ru_n(TPPZ)_{n+1}]^{2n+}$ complexes show a main absorption band in the visible region whose maximum shifts to lower energies as n is increased (see Figure 1). Associated with this energy shift, an increase in the intensity of the main spectral feature (Ia in Figure 1) is observed, with relative intensities (referred to that of the monomer spectrum) of 2.2 ($n = 2$) and 2.7 ($n = 3$), see Table 1. The main band shows for $n > 1$ a lower energy shoulder below 1.9 eV (Ib in Figure 1), whose intensity increases with n, so that for $n = 5.5$ this feature becomes as intense as the main Ia feature; interestingly, a similar behavior was observed by Bonhôte et al. in dimeric and trimeric Ru(tetrapyridophenazine) complexes.[42] Below 1.4 eV, the band tail (Ic in Figure 1) is found.

The computed spectra of the $n = 1-4$ oligomers in the visible energy region are shown in Figure 6. The positions of the main absorption peaks agree very well with the experiment, with a deviation of 0.27 eV, at most, observed for the trimer. In particular, the observed red-shift and intensity increase of the main Ia feature with increasing n are well-described by the calculations (see Table 1). Also well-described are the Ic tails in the region below 1.4 eV. Instead, the Ib shoulder of the main visible band for $n > 1$ is not reproduced by our calculations. This discrepancy cannot be related to an effect due to the limited basis set expansion, since we found the Ib feature to be entirely missing also in the dimer spectrum computed with the larger LANL2DZ basis set. A more detailed discussion of the Ia, Ib, and Ic features is given below.

Ia Feature. We assign the most intense band in the visible region to an MMLCT multitransition from the Ru t_{2g} HOMOs

(42) Bonhôte, P.; Lecas, A.; Amouyal, E. *Chem. Commun.* **1998**, 885.

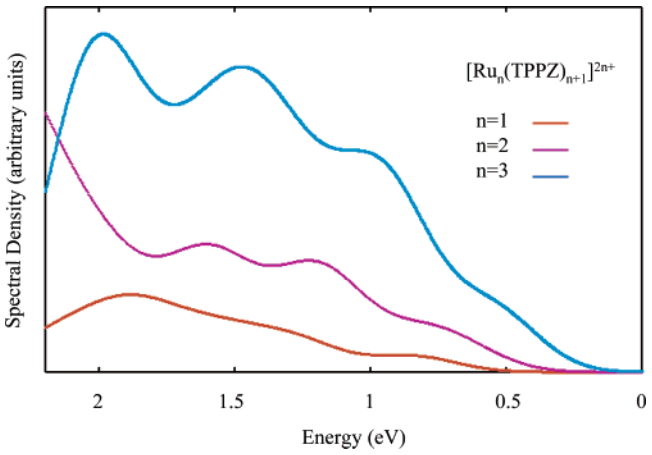

Figure 7. Singlet−triplet spectral density for the $[Ru_n(TPPZ)_{n+1}]^{n+}$ complexes with $n = 1$ (red line), 2 (violet line), and 3 (blue line) in the region 2.1−0 eV.

to π^* orbitals delocalized over both the pyrazine and pyridyl ligands, spanning the entire molecular system. As for the monomer, the most intense transitions show a sizable amount of metal character in the final states. For the dimer, the arriving states of the most intense transitions are t_{2g}-π^* antibonding combinations localized on the central (orbital 347) and terminal (orbitals 350−351) pyrazines (see Figure 4), and therefore the resulting excited state, being a superposition of these three t_{2g}-π^* states, is delocalized over the entire molecule. Similarly, for the trimer (tetramer) the final state of the most intense multitransition in the main visible absorption band is a superposition of t_{2g}-π^* combinations, orbitals 470−471 (591−595), involving pairs of contiguous metal centers. This indicates that the TPPZ units of the oligomeric species communicate through the intermediacy of the metal centers and of the central pyrazine bridges, to form excited states delocalized throughout the entire complex.

Ic Feature. The less intense transitions computed below 1.4 eV, which give rise to the experimentally observed band tail of the dimer and trimer spectra, are found to have pure MLCT character: they originate from the ruthenium t_{2g} orbitals, but the final states are symmetrically localized on the central pyrazine ligands, with small or no metal character. The lower intensity of these transitions can therefore be related to the absence of metal character in their final states and to a reduced charge transfer with respect to the main spectral features, which are delocalized over all the TPPZ ligands.

Ib Feature. To gain insight into the origin of the low energy shoulders which appear in the oligomers experimental spectra below 2.0 eV (620 nm in Figure 1), we analyzed in detail the spectral density of singlet−triplet (S−T) transitions for the investigated $[Ru_n(TPPZ)_{n+1}]^{2n+}$ complexes with $n = 1, 3$. At our level of theory, these spin-forbidden transitions do not contribute to the calculated absorption spectrum, i.e., they have zero oscillator strength, because spin−orbit interactions are not included in our calculations. In Figure 7, we report the S−T spectral density for the $[Ru_n(TPPZ)_{n+1}]^{2n+}$ complexes with $n = 1-3$, computed assuming an arbitrary unitary oscillator strength for each transition. A high spectral density of S−T transitions is clearly seen in the region below 2.0 eV, where the experimentally observed shoulders are present for the species with $n > 1$. These transitions appear to have the same MMLCT and MLCT character of the corresponding singlet−singlet ones discussed above. Moreover, the S−T spectral density increases with n and is distributed around the same energy range for all the investigated species, in agreement with the experimental spectra. Thus, these results suggest that the Ib shoulders are due to spin-forbidden MMLCT and MLCT singlet−triplet transitions. We note indeed that a recent ab initio study of the $[(NH_3)_5Ru(4,4'\text{-bypyridine})Ru(NH_3)_5]^{4+}$ dimeric Ru(II) species in solution[22] has shown that taking into account spin−orbit interactions through a phenomenological coupling leads to an intensity borrowing from the singlet to the triplet MLCT states, which introduces a shoulder of the main singlet absorption feature 0.4 eV below it.[22]

The interpretation of the Ib feature in terms of S−T transitions is supported by the experimental visible spectra of the corresponding $[Os_nTPPZ_{n+1}]^{2n+}$ complexes with $n = 1-3$ (Supporting Information), which show a considerable enhancement of the lower energy features with respect to the Ru complexes spectra. Indeed, because of the higher atomic number, spin−orbit interactions are expected to increase going from Ru to Os compounds, so that singlet−triplet transitions should appear with enhanced intensity in the Os compounds spectra. In particular, the monomeric Os species shows quite an intense band centered around 1.9 eV, which is entirely missing in the corresponding Ru system. Consistent with this experimental observation, a spin-forbidden (zero oscillator strength) band is found to be present in the Ru monomer complex spectrum at ∼1.9 eV (see Figure 7).

C. Effective Conjugation Length. A property of considerable interest in the study of coordination polymers is the effective conjugation chain length.[12] The ECL is associated to the extent of spatial conjugation in π-conjugated systems which is generally maximized when the communicating subunits show a coplanar arrangement. In the investigated $[Ru_n(TPPZ)_{n+1}]^{2n+}$ complexes, the Ru octahedral coordination imposes an orthogonal arrangement of the two TPPZ ligands bound to each metal center, so that an ECL restricted to a single or at most to a few TPPZ units might be expected. Following a standard procedure,[12] in Figure 8 we plot the theoretical and experimental peak energies, E_{max}, for band Ia as a function of the inverse number of TPPZ ligands, $1/(n + 1)$; for comparison, in the same figure the computed HOMO−LUMO gap energies (dotted line) are also shown. It appears that, within the investigated range of TPPZ units, both computed and measured E_{max} show an approximately linear behavior, and although the agreement between these two lines—very satisfactory for the monomer—becomes slightly worse with increasing n, the difference between their estimated limiting values for large n, 1.77 and 1.35 eV, is still reasonable. It also appears that the data in Figure 8 show no saturation effect that could be used to define the ECL, implying that an ECL of several (>6.5) TTPZ units is actually present in the Ru−TPPZ complexes. The origin of this remarkable effect is the extended charge delocalization in the excited states, which is observed going from the monomer to the oligomers and is related to intermetal communication through the pyrazine bridges.

Summary and Conclusions

In summary, in this work a class of polynuclear complexes of formula $[Ru_n(TPPZ)_{n+1}]^{2n+}$ (with $n = 1, 2, 3$, and >5) has

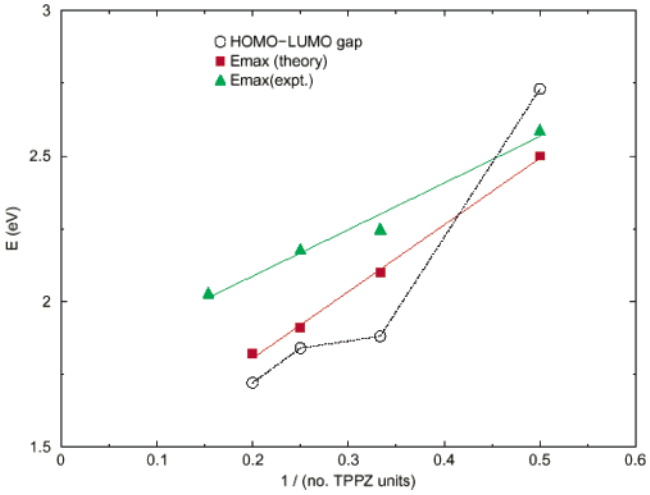

Figure 8. Absorption peaks of band Ia versus the inverse number of TPPZ units in $[Ru_n(TPPZ)_{n+1}]^{n+}$ complexes. Experimental data (green triangles) are for $n = 1-3$, 5.5; theoretical results (red squares) are for $n = 1-4$. The lines which fit the data are $E_{max}(eV) = 1.77 + 1.596/(n + 1)$ and $E_{max}(eV) = 1.35 + 2.293/(n + 1)$, for experiment and theory, respectively. The corresponding limiting values for large n, 1.77 eV (exptl) and 1.35 eV (theor), represent the expected absorption maximum for the polymer, so that E_{max}(polymer)/E_{max}(monomer) = 0.68 and 0.54 according to experimental and calculations, respectively.

been synthesized and spectroscopically characterized. UV−vis spectroscopy shows a red-shift of the main visible absorption band, together with an increase of its intensity, going from the monomer to the oligomeric complexes with higher n. These trends have been analyzed by DFT-TDDFT calculations for the $[Ru_n(TPPZ)_{n+1}]^{2n+}$ complexes with $n = 1-4$. The calculations provide a satisfactory description of the experimental spectra in acetonitrile, particularly of the absorption maxima energies and their relative intensities for different values of n, thus allowing a detailed band assignment for the investigated complexes. The main absorption bands in the visible region of all the investigated species are assigned to as MMLCT from the Ru t_{2g} HOMOs to orbitals of π^* character, which are delocalized over the entire molecular systems with sizable contributions of ruthenium t_{2g} orbitals. For the oligomers, these final states are superpositions of t_{2g}-π^* states which involve pairs of contiguous metal centers and result in excited states delocalized throughout the entire complexes.

The energy features of the oligomers ($n > 1$) spectra below 2.0 eV, which are not reproduced by the computed spectra for singlet−singlet transitions, are proposed to arise from spin-forbidden singlet−triplet transitions which acquire increasing intensity with increasing n. This is supported by the experimental visible spectra of the corresponding $[Os_nTPPZ_{n+1}]^{2n+}$ complexes with $n = 1-3$, which show a considerable enhancement of the lower energy features with respect to the Ru complexes spectra.

The investigation of saturation effects, from both the experimental and theoretical approaches, indicates that an effective conjugation length effect is present in the $[Ru_n(TPPZ)_{n+1}]^{2n+}$ complexes with $(n + 1) > 6.5$. This effect originates from the extended charge delocalization in the excited states going from the monomer to the oligomers and appears to be related to the intermetal communication through the pyrazine bridges.

The present study demonstrates that the interplay between theory and experiment is capable of providing useful insights to the understanding of the electronic and optical properties of complex coordination polymers.

Acknowledgment. This work was partially supported by NSF through Grant DMR-0213706 to the MRSEC-Princeton Center for Complex Materials. S.B. gratefully acknowledges support from a Camille and Henry Dreyfus Foundation New Faculty Award.

Supporting Information Available: Experimental section. NMR spectra of $[Ru_n(TPPZ)_{n+1}]^{2n+}$ with $n = 1$, 2, 3, and >5. Molecular structures. Comparison between $[Ru_n(TPPZ)_{n+1}]^{2n+}$ and $[Os_n(TPPZ)_{n+1}]^{2n+}$ ($n = 1-3$) spectra. Car-Parrinello and G03 $[Ru_2(TPPZ)_3]^{2+}$optimized geometries. Comparison of the monomer and dimer spectra obtained using the LANL2DZ and STO-3G basis sets. Optimized geometrical parameters of $[Ru_n(TPPZ)_{n+1}]^{2n+}$ ($n = 1-4$). Energies and composition of the frontier orbitals of the $[Ru_n(TPPZ)_{n+1}]^{2n+}$ complexes ($n = 1-4$) in solution. Excitation energies, oscillator strengths (f), and composition of the TDDFT eigenvectors for $[Ru_n(TPPZ)_{n+1}]^{2n+}$ ($n = 1-4$) in solution. This material is available free of charge via the Internet at http://pubs.acs.org.

JA048421U